IOP Conf. Series: Materials Science and Engineering **284** (2017) 012026 doi:10.1088/1757-899X/284/1/012026

Development of corrosion resistant surfaces via friction stir processing for bio implant applications

Gurvinder Pal Singh Sodhi[1,3] and Harpreet Singh[1]
[1]Department of Mechanical Engineering, Indian Institute of Technology Ropar Rupnagar, Punjab, India
3Corresponding author email gurvinderpss@iitrpr.ac.in

Abstract. Current investigation presents the use of Friction Stir Processing (FSP) to improve the corrosion resistance of pure magnesium for biomedical applications. FSP has been used to incorporate hydroxyapetite (HAP) into Mg-surface so as to modify the chemical composition. FSP was done within a matrix of different parameters and conditions. Influence of various parameters on microstructure was also clearly observed. XRD analysis confirmed the presence of HAP, whereas SEM images revealed a uniform distribution of the imbedded phase. Micro-hardness and in-vitro corrosion studies were also performed. Influence of grain size on hardness was validated by Hall-Petch relationship. Corrosion behavior was explained on the basis of texture, which indicated better corrosion resistance in comparison to the pure Mg. Therefore, the study reveals that the proposed FSP methodology can be useful tool to improve mechanical and corrosion properties of pure Mg for biomedical applications.

1. Introduction

Biodegradable metals and alloys are being considered as the second generation of biomaterials. In this context, due to its close resemblance with the human bone in terms of mechanical properties, Mg has the potential to be amongst one of the best materials, which can be incorporated in human body. However, its rapid degradation is still a matter of serious concern. Many researchers [1-2] have been trying to address the problems pertaining to hydrogen evolution and high corrosion rates of Mg implants. According to literature [3], Mg implants are being widely used as cardiovascular stents, fixation plates etc. Due to the fact that, the properties of Mg can be engineered easily, it is highly beneficial to use it for customized biomedical applications. In this context, (FSP) approach has been chosen, which is a solid state process wherein the material is subjected to intense plastic deformation by a rotating tool. This in turn refines the grain structure of the metal/alloy by re-crystallization. In the recent past, agglomeration and uneven distribution of HAP powder in pure Mg during friction stir processing, have been identified as the key problems to be addressed [4-5]. It has been concluded that by playing with the FSP parameters and conditions, and/or by using various tool shapes, one can achieve the desired grain size and uniform distribution of secondary phase in the processed metal [6]. Mishra et al [7] in a review article, laid emphasis on mechanisms responsible for microstructural refinement, and effects of FSW/FSP parameters on resultant microstructure and final mechanical properties. Kang et al [8] reported, that grain refinement, homogeneity as well as porosity free microstructure can be achieved by FSP. Although literature reports various techniques other than FSP, such as laser cladding for improving wear and corrosion resistance properties of magnesium and its alloys, however cost and time are the important factors which are compromised [9]. There are some attempts to use cold spray technology also to modify the Mg-surfaces, for example depositing aluminum cold spray coatings on Mg-substrates, however premature corrosion and toxicity of aluminum poses a serious threat to use Al in human body [10]. Gray and Luan [11] in their review

articles, have concluded that various other surface coating techniques such as electrochemical plating (electroplating), conversion coatings, anodising, hybrid coatings, microarc oxidation and vapour-phase processes, have been considered for Mg alloys. All these surface modifications are either giving moderate corrosion resistance or slight changes in hardness, due to this fact they are not suitable for use in biomedical applications. Few researchers have tried to add TiC nanoparticles to magnesium alloy for strength and ductility enhancement and reported changes in microstructure which led to enhancement of tensile properties [12]. Although FSP alone can have significant effect on grain refinement, wear resistance, hardness, mechanical behavior of Mg alloys, however standalone Mg is not suitable for body implants, due to poor electrochemical performance. Thus comes an idea of incorporation of Hydroxyapatite (HA) particles ($Ca_5(PO_4)_3(OH)$) into the metal. An extensive review of the microstructural evolution during FSP and the effects of processing parameters is available [13]. It is largely accepted that dynamic recrystallization (DRX) governs grain refinement in FSP [14-17], although there is still a debate over the exact mechanisms that govern the resultant microstructure. Taking the advantage of available literature and research findings. FSP with a novel method of incorporating secondary phase has been used in this study.

2. Experimental details

Commercially pure magnesium ingot (Purity 99.9%) purchased from National Aerospace Laboratory Bangalore (India) was used as base material in this study. Hydroxyapatite powder (HA) was used as reinforcement to make a composite layer via FSP route. The HA was purchased from Sigma Aldrich with particle size in the range 25–60 μm . Fig. 1 & 2 show XRD analysis of pure magnesium and HA powder respectively.

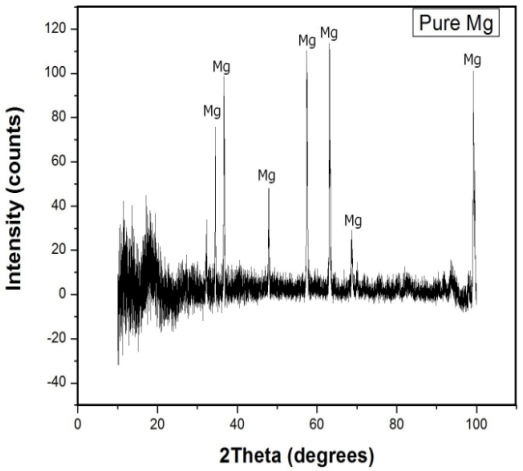

Figure 1. XRD analysis of pure magnesium**.**

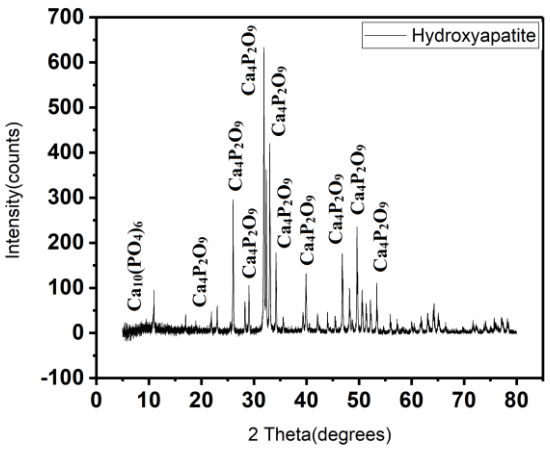

Figure 2. XRD analysis of HAP powder.

Three samples coupons (80 × 40 × 6 mm) of magnesium were cut by Abrasive Jet Cutter (Make: Chennai Metco; Model: Bainmount; India) for FSP. During FSP, the sample was fixed in FSP fixture, as shown in Fig.3. A conical shaped tool made from stainless steel of grade 202 was used for FSP. The tool had threads on its pin with shoulder diameter of 18mm, a tool-tip length 3 mm (Fig. 3). An improved material flow takes place in the samples processed with the tool consisting of a threaded pin due to downward movement of the material [18-19]. The workpieces were friction stir processed (FSPed) using 1 pass under constant rotational (w) and traverse (v) speeds of 2000 rpm and 60 mm/min respectively. The samples have been designated as per the nomenclature given in Table 1.

Table 1. Nomenclature of samples used in this study.

Designation	Description of processing
Mg	As-cast pure Magnesium without FSP
F-Mg	As-cast Magnesium subjected to FSP
F-Mg-H	As-cast Magnesium subjected to FSP with HAP as re-inforcements

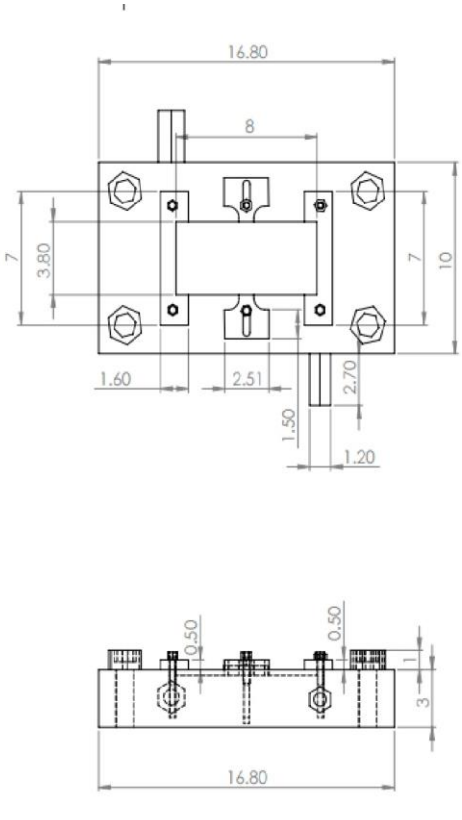

Figure 3. Schematic of fixture to hold Mg pieces for friction stir processing.

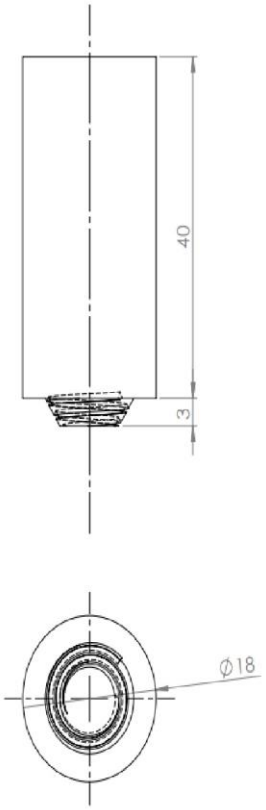

Figure 4. Sketch of conical tool used for friction stir processing of Mg.

To address the problems of agglomeration and non-uniform distribution of HAP powder in Mg substrate, a novel approach to fill HAP powder inside the sample has been proposed and utilized. A hole was drilled (vertically-2.5mm dia) throughout the length of the coupon, in which HAP powder (0.01% vol fraction was filled). Both sides of the hole were sealed by using a suitable fastener. This method of injection resulted in nearly zero wastage of powder, which is usually not achievable in any other methods of filling reinforcements during FSP. Fig. 5 shows the schematic illustration of the approach used for FSP.

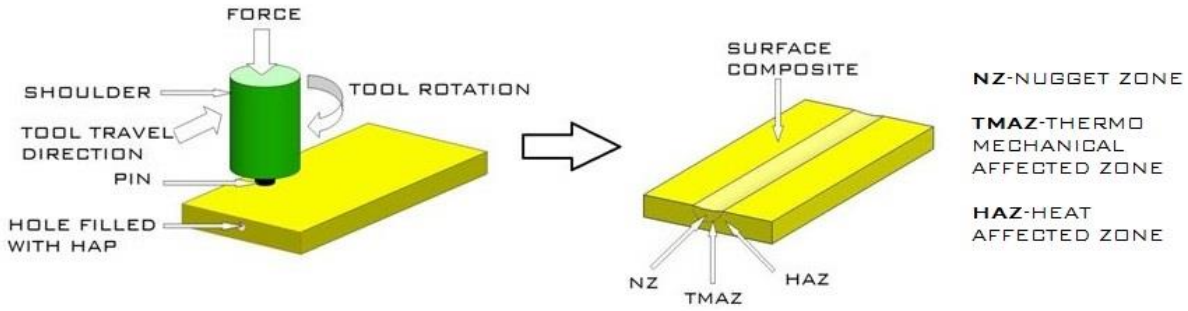

Figure 5. Schematic illustration of the complete FSP process, used to make Mg- composites reinforced with hydroxyapetite.

For the analysis of microstructure and mechanical properties, the FSPed samples were sectioned and mounted in transoptic powder at a hot mounting machine (Make: Chennai Metco; Model: Bainmount; India). Mirror polishing of the mounted samples was done by using standard metallographic procedure. For optical microscopy, etching was done with a solution consisting of 2.5 ml acetic acid, 1.5 ml picric acid, 2.5 ml acetic acid, 15 ml water and 50 ml ethanol. The cross-sections were examined using a Leica Microscope (Make: Leica Microsystems; Model: MEF4M; Germany) optical microscope. Subsequently, micro hardness measurements were made using a Hardness Tester (Make: Wilson Instruments; Model: 402 MVD; USA). Vickers indentor with a test force of 1 Kg and dwell time of 15 seconds was used. X-ray diffraction (XRD) analysis of FSPed samples was carried out using a PANalytical X-Pert Pro machine (Make: PANalytical; Model: X-Pert Pro; The Netherlands). All the XRD scans were carried out with a step size of 0.04° (2θ) and a sampling time of 3 s per step in 2θ range of 0°-180°. Scanning electron microscope (SEM), (Make: Jeol; Model: JSM6610LV; USA) equipped with energy dispersive spectroscopy, EDS (Make: Oxford, Model: INCAX-Act, USA) was used to characterize morphology and composition of the sectioned samples.
An Electrochemical Cell (Make: Gamry; Model: PTC1; USA) was used to perform in-vitro potentiodynamic studies, of three standard electrode configurations; Calomel electrode as reference electrode, Graphite electrode as counter electrode and test specimen as working electrodes. Mg, F-Mg and F-Mg-H samples were subjected to potentiodynamic polarization after 1 hr and 25 hr immersion in the Hank's solution, to stabilize the corrosion rate. The scan rate was 0.1mV/s and applied potential was varied ±0.25 V about the open circuit potential. Initial delay of 1800 seconds was given for each sample before performing the potentiodynamic test. The obtained data was analyzed by Gamry Analyst software. All the tests were performed three times under ambient condition of room temperature (25±1 ℃) and relative humidity (55±5%).

3. Results and discussion

The initial micro structure of the Mg samples comprises large coarse grains with the average grain size of 820 μm (Fig. 6-a). Whereas the microstructure of F-Mg (Fig. 6-b) consists of homogenous and refined grains of about 150 μm average size, which could be attributed to dynamic re-crystallization [20-21]. The interface is shown in (Fig. 6-b) where the refinement is seen. With the rise in temperature and stirring effect while doing FSP finer grains are formed. In the third case, the microstructure of F-Mg–H composites got refined intensely, which is not possible to be revealed by OM (Fig. 6-c).

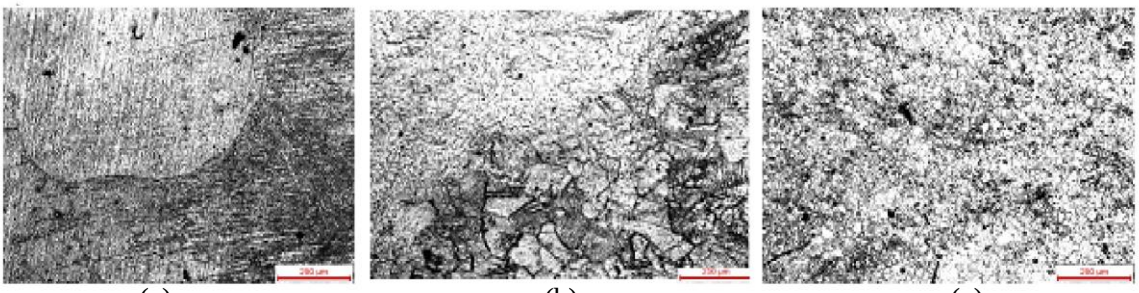

(a) (b) (c)

Figure 6. Cross-sectional optical micrographs of Mg-based surface composites fabricated by single pass of FSP at 2000 r.p.m with a traverse speed of 60 mm/min (a) Mg (b) F-Mg (c) F-Mg-H

The XRD analysis of all the samples is shown in Fig.7. which reveals the presence of Mg as the main phase in all the three cases. In F-Mg no oxidation took place which is a positive attribute. In case of F-Mg-H, elements such as magnesium, phosphorus, calcium and oxygen alongwith additional phases such as calcium phosphate and magnesium phosphate have also been found, which shows the presence of HAP in the sample.

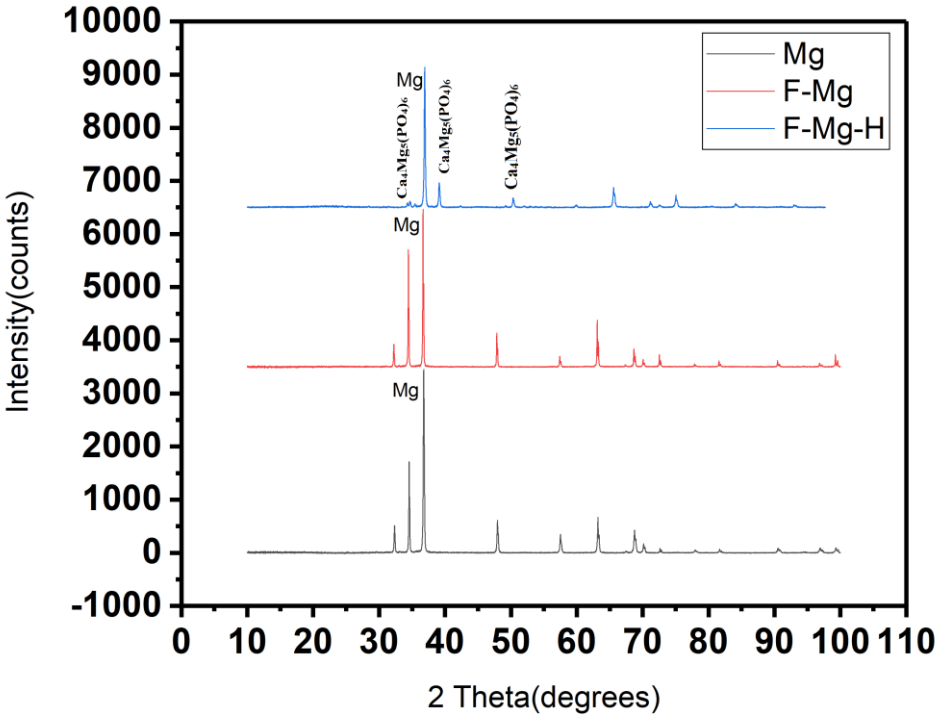

Figure 7. X-Ray diffraction of Mg-based surface composites fabricated by single pass of FSP at 2000 r.p.m with a traverse speed of 60 mm/min.

The cross-sectional SEM micrographs of F-Mg-H samples at different locations are shown in Fig.8, whereas Fig.9 shows the EDS maps of different elements. All the HAP particles are well distributed with the re-crystallized Mg after FSP. This can be attributed to the nature of FSP which forms the composite in solid state itself. Wherein it would have been very difficult to produce composites of Mg with HAP, due to the difference in the melting points of both materials. The element distribution of Mg and HAP particles are clearly seen in Fig. 9. The reinforced particles are dispersed and distributed evenly all over Mg matrix. There is no evidence, during the study, to report presence of clusters,

agglomeration or element rich zones throughout the sample surface. Typical dispersion of HAP particles in the surface composites, ranging from 10-25µ has been recorded. The variation in element distribution in the figure is minimum, which leads to validation of homogenous distribution.

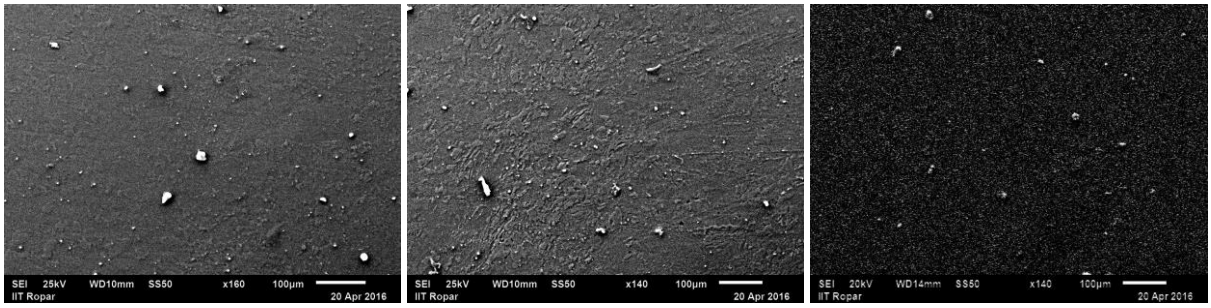

(a) (b) (c)

Figure 8. Cross-sectional scanning electron micrographs of Mg-alloy reinforced with HAP by single pass of friction- stir processing at 2000 r.p.m with a traverse speed of 60 mm/min, showing particle distribution at different locations.

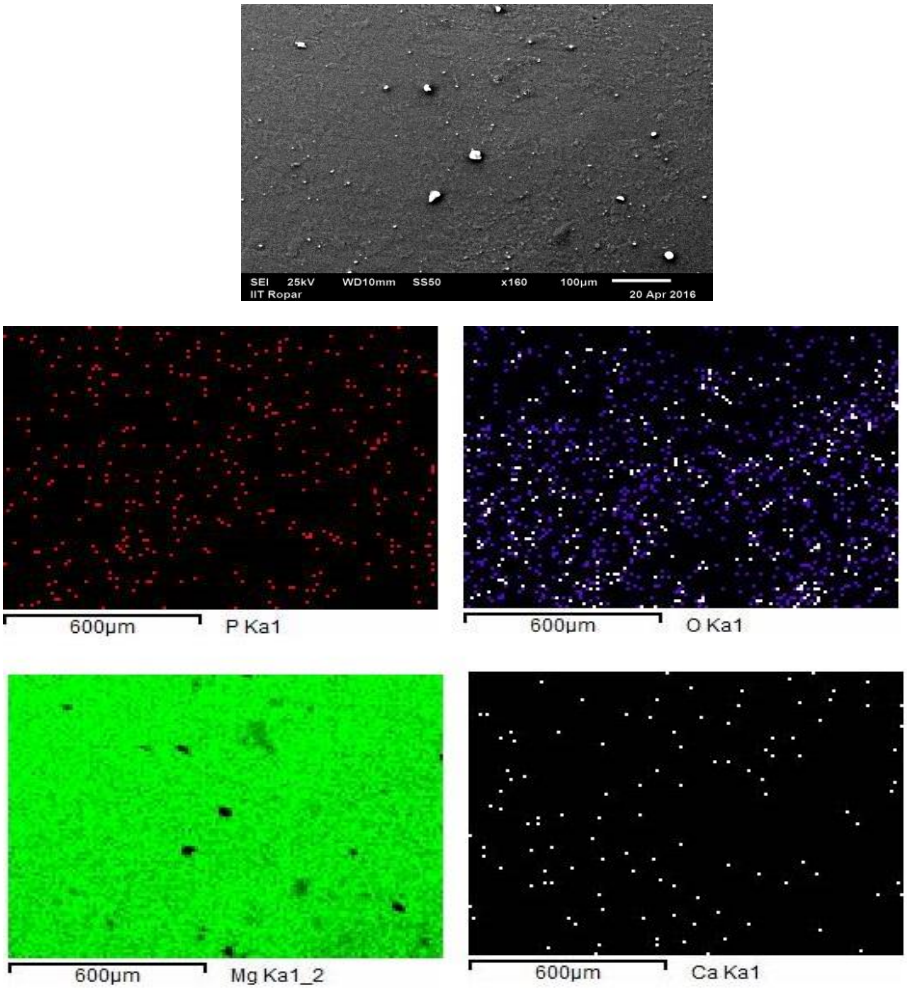

Figure 9. EDS maps of Mg-alloy reinforced with HAP by single pass of friction- stir processing at 2000 r.p.m with a traverse speed of 60 mm/min, showing presence of phosphorous, oxygen, magnesium and calcium after FSP.

The cross-sectional micro-hardness versus distance from the FSP zone- base material interface plots are shown in Fig. 10. The effect of tool rotational speed on the microstructure discussed by various researchers was verified in terms of getting very low surface hardness due to very high heat generations, due to high speeds and prolonged area of contact, which led to grain growth. But eventually when the tool traverse speed was increased it resulted in lower grain size and this higher hardness, which can be observed from the plots of three samples that the variation in micro-hardness is marginal in the base material regions for all the three samples. Higher values of micro-hardness in the heat affected zone (i.e. -25 to +25) were reported for all samples except non-FSPed pure Mg. Whereas as we approach towards the FSP region hardness starts increasing, becomes maximum at a point and then starts decreasing as we move towards the other side of FSP zone. The reason for high hardness in the centre is due to high temperatures in that region which results in dynamic re-crystallization (DRX) and lower hardness on the outer peripheries attributes to larger grain size in that region (due to lower temperature than that in the center) which is in accordance to the Hall–Petch relationship, which states that hardness is inversely proportional to (grain size)$^{1/2}$.The hardness values for all of the Mg/HAP surface composites have narrow distribution ranges, indicating a homogeneous distribution of the HAP phase in the Mg matrix. The average micro-hardness of all the three samples is tabulated below.

Table 1. Average cross-sectional micro hardness of Mg-alloy reinforced with HAP by single pass of friction- stir processing at 2000 r.p.m with a traverse speed of 60 mm/min.

Sr. No.	Sample	Hardness (HV)
1	Mg	36 ±5%
2	F-Mg	43 ±5%
3	F-Mg-HAP	47 ±5%

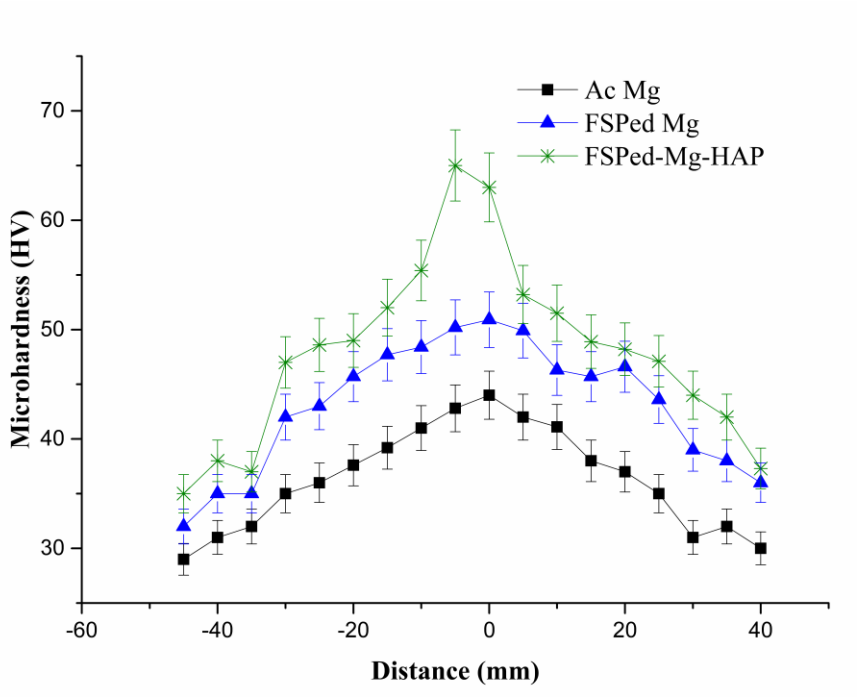

Figure 10. Variation in microhardness along the cross-section of Mg-alloy subjected to Friction Stir Processing (FSP) at 2000 r.p.m with a traverse speed of 60 mm/min.

During the in-vitro corrosion studies, the initial immersion results (Table 2) show equilibrium potential and corrosion rate for Mg, F-Mg and F-Mg-H samples for initial stage i.e 0 hours and after

25 hours. Initial corrosion rates for F-Mg-H (393.9 mpy) were greater than Mg (304.1 mpy), but after 25 hours F-Mg-H (122.9 mpy) shows best corrosion resistant properties, while the F-Mg (304.1 mpy at initial stage and 1529 mpy at 25 hr) shows highest corrosion rates for all time of immersion, which can be attributed to the grain refinement and increased number of grain boundaries. During initial hours of immersion the HAP particles act as cathodic sites on the F-Mg-H surface as a result micro-galvanic coupling occurs between the Mg matrix and HAP particles, similar behavior of micro galvanic coupling has been explained by Song et al [22] for the AZ91 Mg alloy where β particles (Mg17Al12) act as cathodic sites and Mg matrix act as anodic. As reported by Ralston et al [23] grain size of Mg and secondary phase has great significance on corrosion resistance therefore we have reported different corrosion resistances with the explanation of the fact that, due to "dislocation rearrangements" which results due to grain growth after dynamic re-crystallization [24].

Table 2. Equilibrium potential and corrosion rates of Mg-alloy subjected to Friction Stir Processing (FSP) at 2000 r.p.m with a traverse speed of 60 mm/min.

Time	0 hr (Initial)			25 hr (Final)		
Sample	Mg	F-Mg	F-Mg-H	Mg	F-Mg	F-Mg-H
Equilibrium Potential (Vs SCE)V	-1.541	-1.565	-1.564	-1.592	-1.530	-1.546
Corrosion rate (mpy)	304.1	367.7	393.9	165.5	1529	122.9
Icorr A/cm^2	349.8e-6	423.0e-6	453.1e-6	190.3e-6	1.759e-3	141.4e-3
Beta Cathode	364.9e-3	325.4e-3	349.5e-3	310.4e-4	377.7e-3	288.9e-3

4. Conclusion

A corrosion resistant, reinforced Mg composite has been developed via FSP route. With the novel approach in the method of introduction of secondary phase into the Mg has given us positive satisfactory results in terms of uniform distribution of HAP particle into Mg matrix. Improvements in perfect agreement with Hall-Petch relationship were observed which lead to enhancement in mechanical and electrochemical properties. Significant grain refinement has been done, the average grain size has been reduced to 150 μm from 820 μm. Even the hardness of the parent metal has been increased from 36 Hv to 46 Hv, which is attributed to the grain size reduction. Initial corrosion rates for F-Mg-H were greater than Mg but after 25 hours F-Mg-H shows best corrosion resistant properties while the F-Mg (304.1 mpy at initial stage and 1529 mpy at 25hr) shows highest corrosion rates for all time of immersion which can be attributed to the grain refinement and increased number of grain boundaries. FSP combined with innovative ways of incorporation secondary phase in Mg matrix is an effective way to enhance the electrochemical and mechanical properties of pure Mg. These results are of great technological importance since FSP processing can be chosen as a cost effective way to produce composites with adjustable properties.

5. References

[1] Chen, Z., Mao, X., Tan, L., Friis, T., Wu, C., Crawford, R., Xiao, Y., 'Osteoimmunomodulatory properties of magnesium scaffolds coated with β-tricalcium phosphate', *Biomaterials*, **Volume 35**, (2014), pp 8553–8565.

[2] Giridharan, V., Yun, Y., Hajdu, P., Conforti, L., Collins, B., Jang, Y., Sankar, J., 'Microfluidic Platforms for Evaluation of Nano biomaterials: A Review', *Journal of Nanomaterials*, **Volume 2012**, (2012), pp 17.
[3] Song, G., 'Control of biodegradation of biocompatable magnesium alloys', *Corrosion Science*, **Volume 49** (4), (2007), pp 1696–1701.
[4] Khalil, K.A., 'A New-Developed Nanostructured Mg/HAp Nanocomposite by High Frequency Induction Heat Sintering Process', *Int. J. Electrochem. Sci*., **Volume 7** (2012), pp 10698 – 10710.
[5] Suchanek, W.L., Byrappa, K., Shuk, P., Riman, R.E., Janas, V.F., TenHuisen, K.S. 'Preparation of magnesium-substituted hydroxyapatite powders by the mechanochemical–hydrothermal method', *Biomaterials*, **Volume 25**, (2004), pp 4647–4657.
[6] Venkateswarlu, G., Davidson, M.J., Sammaiah, P., 'Effect of Friction Stir Processing Process Parameters on the Mechanical Properties of AZ31B Mg Alloy', *Journal of Manufacturing and Industrial Engineering*, **Volume 13**, (2014), pp 1-2.
[7] Mishra, R., Ma, Z.Y., 'Friction stir welding and processing', *Materials Science and Engineering: R: Reports*, **Volume 50**, (2005), pp 1–78.
[8] Kanga, J., Wilkinsonb, D.S., Mishra, R.K., Yuand, W., Mishra, R.S., 'Effect of inhomogeneous deformation on anisotropy of AZ31 Magnesium sheet', *Materials Science and Engineering: A*, **Volume 567**, (2013), pp 101–109.
[9] Carcel, B., Sampedro, J., Ruescas, A., & Toneu, X., 'Corrosion and wear resistance improvement of magnesium alloys by laser cladding with Al-Si', *Physics Procedia*, **Volume 12**, (2011), pp 353-363.
[10] Champagne, V., Gabriel, B., & Villafuerte, J., 'Cold spray coatings to improve the corrosion resistance of magnesium (Mg) alloys', *Corrosion Prevention of Magnesium Alloys*, (2011), pp 414.
[11] Gray, J. E., & Luan, B., *Journal of alloys and compounds*, 'Protective coatings on magnesium and its alloys—a critical review', **Volume 336** (1), (2002), pp. 88-113.
[12] Paramsothy, M., Chan, J., Kwok, R., & Gupta, M., 'Adding TiC nanoparticles to magnesium alloy ZK60A for strength/ductility enhancement', *Journal of Nanomaterials*, (2011), pp. 50.
[13] Mishra, R. S. and Ma, Z. Y., 'Friction stir welding and processing', *Mater. Sci. Eng., R*, **Volume 50**, (2005), pp. 1–78.
[14] Jata, K. V. and Semiatin, S.L., 'Continuous dynamic recrystallization during friction stir welding of high strength aluminum alloys' , *Scripta Mater*., **Volume 43**, (2000), pp. 743.
[15] Su, J. Q., Nelson, T.W., Mishra, R. and Mahoney. M., 'Microstructural investigation of friction stir welded 7050-T651 aluminium', *Acta Mater*., **Volume 51**, (2003), pp. 713.
[16] Jata, K. V., Sankaran, K.K. and Rushau. J. J., 'Friction-stir welding effects on microstructure and fatigue of aluminum alloy 7050-T7451', *Metall. Mater. Trans. A*, **Volume 31A**, (2000), pp. 218 .
[17] Sato, Y. S., Urata, M. and Kokawa, H., 'Parameters controlling microstructure and hardness during friction-stir welding of precipitation-hardenable aluminum alloy 6063', *Metall. Mater. Trans. A*, **Volume. 33A**, (2002), pp. 625.
[18] Padmanaban, G. and Balasubramanian, V., 'Selection of FSW tool pin profile, shoulder diameter and material for joining AZ31B magnesium alloy–an experimental approach', *Mater. Des*, **Volume 30**, (2009), pp. 2647–2656.
[19] Azizieh, M., Kokabi, A.H. and Abachi, P., 'Effect of rotational speed and probe profile on microstructure and hardness of AZ31/Al 2 O 3 nanocomposites fabricated by friction stir processing', *Mater. Des*, **Volume 32**, (2011), pp. 2034–2041.
[20] Forst, H. J., and Ashby, M. F., 'In: Deformation-mechanism maps', Oxford: Pergamon Press, (1982), pp. 21–44.
[21] Jata, K. V., and Semiatin, S. L., 'Continuous dynamic recrystallization during friction stir welding of high-strength aluminum alloys', *Scripta. Mater*., **Volume 43**, (2000), pp. 743–749.

[22] Song, Y., Shan, D., Chen, R., Zhang, F. and Han, E.H., 'Biodegradable behaviors of AZ31 magnesium alloy in simulated body fluid', *Mater. Sci. Eng. C*, **Volume 29**, (2009), pp. 1039–1045.
[23] Ralston, K. and Birbilis, N., 'Effect of grain size on corrosion: a review', *Corrosion*, **Volume 66**, (2010), pp. 75005–75013.
[24] Ben-Haroush, M., Ben-Hamu, G., Eliezer, D. and Wagner, L., 'The relation between microstructure and corrosion behavior of AZ80 Mg alloy following different extrusion temperatures', *Corros. Sci*. **Volume 50**, (2008), pp. 1766–1778.

Acknowledgements
Authors are highly thankful to Indian Institute of Technology, Ropar, Punjab, India for its continuous financial support.